Particuology 115 (2026) 378–389

Contents lists available at ScienceDirect

Particuology

journal homepage: www.elsevier.com/locate/partic

A study on the discharge and mixing process of wet coal in silos

Haoyuan Li, Kaixin Dai, Jun Xie*, Xiaole Chen, Dong Li, Xiaojian Xie, Chuanwen Zhao

School of Energy Science and Engineering, Nanjing Normal University, Nanjing, 210023, China

HIGHLIGHTS

- Develops a CG-DEM model coupled with moisture-induced cohesive force.
- Reveals the decisive influence of stacking sequence on the evolution of outlet coal quality.
- Quantifies that cohesive force dominates, affecting ~80% of particles throughout discharge.
- Demonstrates that flow is characterized by a lower-layer-dominated funnel flow pattern.
- Provides a high-fidelity, low-cost tool for predicting industrial wet coal discharge.

GRAPHICAL ABSTRACT

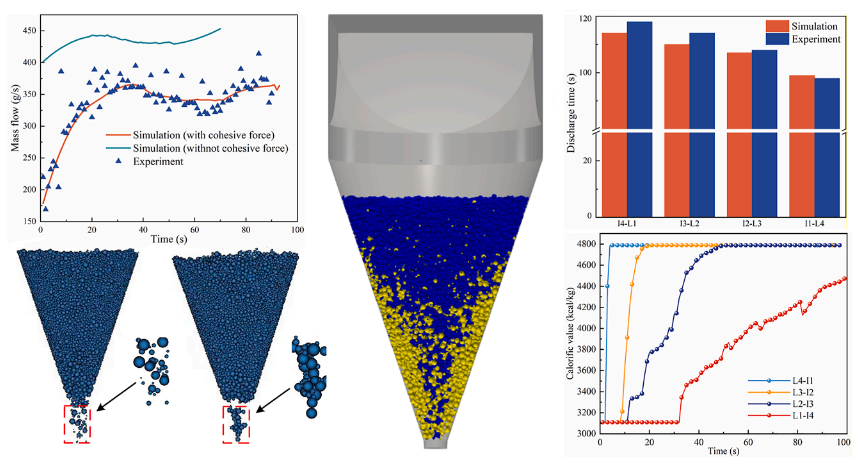

ARTICLE INFO

Keywords:
Silo
Wet coal
Mixed discharge
CG-DEM
Cohesive force

ABSTRACT

This paper develops a computational framework coupling a moisture-induced cohesive force model with the Coarse-Grained Discrete Element Method (CG-DEM) to efficiently and accurately simulate the mixed discharge process of wet coal in a laboratory-scale three-dimensional silo. The moisture-induced cohesive force model quantifies the effect of moisture on coal flowability by correlating moisture content with macroscopic mechanical parameters of the particles (cohesion, internal friction angle). Simulation results indicate that particle flow exhibits a significant central-channeling "funnel flow" characteristic, and the flow structure is dominated by the flowability of the lower coal layer. The moisture-induced cohesive force is a key factor controlling particle motion. The study further reveals the decisive influence of stacking sequence on the evolution of outlet coal quality: when the lower layer consists of high-moisture, poor-flowability Indonesian coal, the outlet calorific value shows a slow rising trend; conversely, when the lower layer consists of good-flowability Longwanggou coal, the outlet calorific value decreases rapidly. This research provides a reliable, low-cost numerical tool for understanding and predicting the discharge and mixing behavior of wet coal in industrial silos, offering guidance for optimizing coal blending and stabilizing the quality of feed coal.

* Corresponding author.
E-mail address: junxie@njnu.edu.cn (J. Xie).

https://doi.org/10.1016/j.partic.2026.06.007
Received 31 March 2026; Received in revised form 28 May 2026; Accepted 7 June 2026
Available online 13 June 2026
1674-2001/

1. Introduction

Driven by economic constraints and the demands of peak-shaving operations, coal-fired power plants are often precluded from relying on a single coal type for long-term generation. Multi-coal blending combustion has become the norm. Under blending conditions, the layered stacking and discharge in silos lead to fluctuations in the mass ratio and calorific value of the blended coal at the outlet over time. However, limited by on-site conditions, the internal flow within the silo and the composition of the outlet coal mixture are difficult to monitor, thereby increasing uncertainty in stable combustion and load regulation of the unit. Numerical simulation has become an effective research method. The Discrete Element Method (DEM) can directly solve the motion process of individual particles, thus showing significant advantages in describing the flow, mixing, and adhesion of coal particles. However, the computational cost of DEM increases linearly with the number of particles. Actual industrial silos often contain particle systems of extremely high orders of magnitude, making DEM simulation difficult to complete within acceptable computational cost and time (Queteschiner et al., 2018; Zhong et al., 2016). Furthermore, due to the adhesive and multiphase properties of wet coal, specifically the cohesive bridging effects driven by moisture, a single simplified model is insufficient to fully characterize the system. It is essential to constrain model assumptions and parameter applicability ranges through direct comparison with experimental data. Consequently, developing a cost-effective, high-fidelity mathematical model capable of capturing the adhesive effects of wet coal particles is crucial for realistically simulating mixed discharge in silos. This endeavor addresses critical research gaps and serves as a prerequisite for achieving precise design and optimized operational control.

Researchers have employed various methods such as experiments and numerical simulations to explore particle flow in silos from multiple levels. The research extensively covers the influence laws of silo geometric structure (e.g., cone angle (Jung et al., 2012; Wang et al., 2020), eccentric design (Hao et al., 2026; Jiang, Ma, et al., 2026; Wu et al., 2025), outlet size (Lu, Guo, et al., 2017), internal inserts (Lu et al., 2023; Yuan et al., 2020)), material properties (e.g., particle shape (Hanif et al., 2025; Höhner et al., 2012; Zhang et al., 2021), particle size distribution (Deng et al., 2020; Zhao et al., 2017)), and external intervention conditions (e.g., aeration (Chen et al., 2011; Lu et al., 2012), vibration (Kumar et al., 2020; Wassgren et al., 2002)) on phenomena such as discharge mode, flow rate, particle segregation, arching, and blockage. However, most of the above studies are limited to dry particles, with very few focusing on wet particles. A small number of studies have made progress in predicting the discharge flow of wet particles, but there is still a lack of high-fidelity 3D DEM simulation and in-depth mechanistic research on the mixing behavior of wet coal particles in industrial-scale 3D silos during dynamic discharge. For instance, Dai et al. (2021) studied the discharge characteristics of wet coal through silo experiments and a continuum model. The study pointed out that when the moisture content is low, coal particles have better flowability. When the moisture content increases, significant cohesive behavior appears, the mass flow rate decreases accordingly, the velocity difference between particles in the center and near the wall intensifies, making wet coal more prone to funnel flow, thereby bringing higher risks of arching and instability. Subsequently, Dai et al. (2024) further focused on the discharge and mixing of multi-component wet coal in silos. The study found that moisture content, silo half-angle, and discharge rate jointly alter the flow pattern, affect the magnitude of the mass flow rate, and directly influence the evolution of outlet composition over time. Recently, Zhu et al. (2024) focused on the effect of vertical vibration on the discharge process of cohesive fine powder in a silo. Combining experiments and DEM simulation, the study found that the vibration acceleration amplitude is the key parameter triggering arch formation, with little relation to vibration frequency. Anand et al. (2009) earlier used the Discrete Element Method (DEM) to predict the discharge dynamics of wet cohesive particles from a 2D rectangular silo. The study quantified inter-particle cohesive force by introducing a pendular liquid bridge model. Subsequently, Anand et al. (2015) further systematically validated the aforementioned DEM model predictions through experiments. The study measured discharge rate, angle of repose of residual material after discharge, and the size of agglomerates formed during discharge.

There are various methods to improve the simulation efficiency of DEM, such as reducing particle stiffness (He et al., 2021), GPU parallel acceleration computing (Gou & Shen, 2025), and the coarse-grained method (Ren et al., 2025). In comparison, the coarse-grained method can maintain high simulation accuracy while avoiding extensive hardware resource usage, and has become an effective method for simulating large-scale particle systems. The Coarse-Grained Discrete Element Method (CG-DEM) can reduce the computational scale through a coarse-grained strategy while retaining the discrete characteristics of particles and the contact dynamics mechanism, to meet the computability of multi-particle systems within an engineering time scale. Simultaneously, a moisture-dependent cohesive force model is introduced to characterize the adhesive effects between wet coal particles, thereby more realistically reproducing the channeling, stagnation, and mixing behaviors of different coal types during the discharge process.

This paper combines the moisture-induced cohesive force model with CG-DEM to conduct numerical simulation research on the layered discharge process in a laboratory silo. First, the scaling factor and cohesive force model are validated; then, the simulation results of the outlet mass flow rate and estimated calorific value are compared with experimental results, confirming the applicability of the coupled model; finally, simulations of the mixed coal discharge process at laboratory scale are conducted. The distribution and evolution of key parameters such as flow pattern, velocity, cohesive force, and calorific value are analyzed.

2. Mathematical model

2.1. Coarse-grained model

As shown in Fig. 1, a single coarse-grained unit represents a particle cluster composed of n^3 original particles, with geometric dimensions n times that of the original particles. This scaling strategy fundamentally reduces the total number of particles in the system, effectively improving computational efficiency (Sakai & Koshizuka, 2009).

The calculation formulas for the diameter and mass of the coarse-grained particles (CGP) are as follows:

$$m_{CGP} = k^3 m_p \tag{1}$$

$$d_{CGP} = k d_p \tag{2}$$

where m_{CGP} and m_p are the masses (kg) of the coarse-grained and actual particles, respectively; d_{CGP} and d_p are the diameters (m) of the coarse-grained and actual particles, respectively; k is the scaling factor.

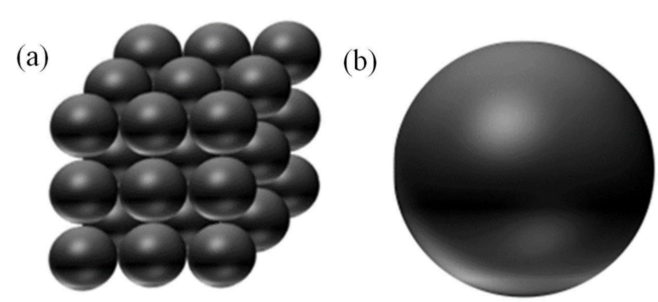

Fig. 1. Coarse-grained model ($k = 3$): (a) Original particles and (b) Coarse-grained particles.

In CG-DEM, the motion of each coarse-grained particle is governed by Newton's second law. The translational and rotational governing equations are as follows (Wang & Shen, 2022):

$$m_{CGP}\frac{dv_{CGP}}{dt} = m_{CGP}g + F_{c,CGP} + F_{L,CGP} \tag{3}$$

$$I_{CGP}\frac{d\omega_{CGP}}{dt} = T_{CGP} \tag{4}$$

where $F_{L,CGP}$ is the cohesive force; I_{CGP} is the particle's inertia tensor; g is the gravitational acceleration (m/s^2); dv_{CGP}/dt is the particle's translational acceleration (m/s^2); $d\omega_{CGP}/dt$ is the particle's angular acceleration (rad/s^2); v_{CGP} and ω_{CGP} are the particle's translational and angular velocities (m/s, rad/s); $F_{c,CGP}$ and T_c are the collision force and torque.

T_{CGP} is given by:

$$T_{CGP} = \sum_{j=1,j\neq i}^{N}\left(Ln \times F^{t}_{c,CGP}\right) \tag{5}$$

where L is the distance (m) from the particle center of mass to the contact point; N is the number of all particles colliding with the current particle; $F^{t}_{c,CGP}$ is the tangential collision force (N) between particles.

$F_{c,CGP}$ is calculated as follows (Cundall & Strack, 1980):

$$F_{c,CGP} = F^{n}_{c,CGP} + F^{t}_{c,CGP} \tag{6}$$

where $F^{n}_{c,CGP}$ and $F^{t}_{c,CGP}$ represent the normal and tangential collision forces (N) between particles, respectively, as shown below:

$$F^{n}_{c,CGP} = -(k_n\delta_n + \eta_n\dot{\delta}_n)n \tag{7}$$

$$F^{t}_{c,CGP} = \min\left[(-k_t\delta_t + \eta_t\dot{\delta}_t)t, \mu_s F^{n}_{c,CGP}\right] \tag{8}$$

where n and t are the unit normal and tangential vectors from the center of mass of particle i to that of particle j; k_n, k_t are the elastic coefficients; η_n, η_t are the damping coefficients; δ_n, δ_t are the thicknesses of the overlap region; the dot over δ denotes the derivative with respect to time.

The Linear-Spring-Dashpot (LSD) soft-sphere collision model is used. In the LSD model, when a collision occurs between particle i and particle j, the relationship between the normal damping coefficient $\eta_{n,p}$ and the normal restitution coefficient $e_{n,p}$ is as follows:

$$e_{n,p} = \exp\left(\frac{\eta_{n,p}t^{col}_{n,p}}{2m_{eff,p}}\right) \tag{9}$$

where $m_{eff} = m_j m_i/(m_i + m_j)$ is the effective mass of the particles, $t^{col}_{n,p}$ is the collision time of the particles, which can be expressed specifically as follows (Garg et al., 2012):

$$t^{col}_{n,p} = \pi\left(\frac{k_{n,p}}{m_{eff,p}} - \frac{\eta^2_{n,p}}{m^2_{eff,p}}\right)^{-1/2} \tag{10}$$

Based on different criteria, various scaling laws have been proposed to scale collision parameters from original particles to CGP. In most studies, it is assumed that the elastic constant and friction coefficient of CGP are the same as those of the original particles ($k_{n,cgp} = k_{n,p}$; $\mu_{cgp}=\mu_p$). Aggregating original particles into CGP reduces the collision frequency, which directly affects energy dissipation. To account for this error, an effective restitution coefficient e_{CGP} is used by assuming equal energy dissipation during collision between the original and coarse-grained systems. Its calculation formula is as follows (Hilton & Cleary, 2014; Lu, Konan, & Benyahia, 2017):

$$e_{CGP} = \sqrt{1 + \left(e^2_p - 1\right)k} \tag{11}$$

The normal damping coefficient in the coarse-grained model is given by:

$$\eta_{n,CGP} = \sqrt{2k_n m_{CGP}}\ \frac{|\ln e_{CGP}|}{\sqrt{\pi^2 + \ln^2 e_{CGP}}} \tag{12}$$

2.2. Moisture-induced cohesive force model

The moisture-induced cohesive force, highly related to water content, significantly affects the flowability of pulverized coal. As previous studies have shown (Lu et al., 2018), the cohesive behavior of pulverized coal exhibits distinct characteristics due to its non-spherical, polydisperse particles, making simplified theoretical liquid-bridge models less accurate for this system. The cohesive force can be correlated with moisture content using the method proposed by Rumpf and Molerus. The relationship between the moisture-induced cohesive force F_L (N) and σ_t is derived as follows (Molerus, 1975; Rumpf, 1970):

$$F_{L,CGP} = k^3 F_L \tag{13}$$

$$F_L = d^2_{sv}\sigma_t\varepsilon/(1-\varepsilon) \tag{14}$$

where, σ_t is the tensile strength (kPa); the Sauter mean diameter (d_{SV}) and the particle size distribution of the coal powder are measured by sieving, and the results are shown in Fig. 2.

The bed porosity (ϵ) is defined as the sum of the gas and liquid volume fractions, expressed as:

$$\varepsilon = 1 - \frac{\rho_b}{\rho_p} \times \left(1 - \frac{M}{100}\right) \tag{15}$$

where ρ_b is the bulk density of the particle bed (kg/m^3), measured by a bulk density tester; ρ_p is the true density of the particles (kg/m^3); M is the moisture content (%), substituted according to the measured value of the experimental coal.

The σ_t can be calculated by the Mohr-Coulomb method, as follows:

$$\sigma_t = C/\tan\Phi \tag{16}$$

where C is the powder cohesion (N), Φ is the internal friction angle, measured by an FT-4 powder rheometer; the specific parameters of the materials used are listed in Table 1. Substituting Eqs. (14) and (15) into Eq. (13) yields the moisture-induced cohesive force for the wet coal particles.

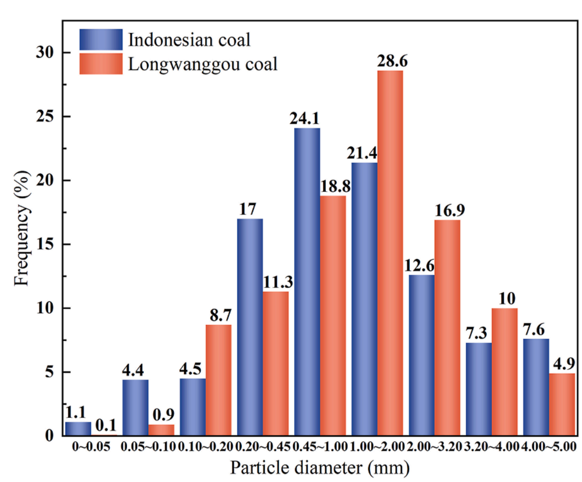

Fig. 2. Particle size distribution.

Table 1
Basic simulation parameter settings.

Parameter	Longwanggou Coal	Indonesian Coal
Average particle diameter (mm)	2.8	3.2
Bulk density (kg/m^3)	778	728
True density (kg/m^3)	1567	1268
Cohesion (N)	0.67	0.68
Internal friction angle (°)	33.4	37.2
Tensile strength (kPa)	1.015	0.895
Moisture content (%)	8.8	35.1
Particle-particle rolling friction coefficient	0.6	
Particle-wall rolling friction coefficient	0.5	
Particle-particle sliding friction coefficient	0.09	
Particle-wall sliding friction coefficient	0.1	
Restitution coefficient	0.1	
Time step (s)	1e-06	

3. Settings

3.1. Experiment conditions

To investigate the discharge process of blended coal from the silo and to provide validation data for the simulation study, an experimental system for the blended coal discharge of Longwanggou coal and Indonesian coal was set up. The mass ratio and mass flow rate of the blended coal at various times were obtained through timed sampling and calorific value testing. As shown in Fig. 3, the system includes components such as a laboratory-scale silo, a feed elevator, a discharge box, and a dust collector. The coal powder is fed into the silo via a conveyor belt, and the discharge is controlled by a valve. The discharge box is used to collect the falling coal powder. To maintain constant moisture content of the coal samples across different experiments, the samples were stored in sealed containers within a constant-temperature refrigerator throughout the process. Each set of experiments was repeated three times, and the results were averaged.

3.2. Simulation conditions

Two coal types, Longwanggou coal and Indonesian coal, were used in the study. The hopper model employed in both experiments and simulations is shown in Fig. 4. The model has a total height of 951 mm, consisting of a conical section with a height of 633 mm, an outlet diameter of 50 mm, and an inlet diameter of 468 mm. Coal powder was placed only within the conical section. The particle size distribution used in the simulations matched the experimental measurements. The conical section was divided equally into five segments along its height, each 123.4 mm tall, labeled H1 (bottom) to H5 (top). Different layered stacking scenarios were realized by controlling the initial filling height ratio of the two coal particles. In the Longwanggou coal-Indonesian coal 3-2(L3-I2) scenario, for instance, Longwanggou coal occupied segments H5 to H3, while Indonesian coal filled segments H2 and H1. Detailed simulation parameters are listed in Table 1.

The simulations in this study were performed using the open-source code MFIX developed by the National Energy Technology Laboratory. The moisture-induced cohesive force model was implemented by modifying the source code. The simulations were conducted on a workstation equipped with dual EPYC 7543 CPUs. The computational domain was meshed, and all simulations were performed in parallel using 48 threads. A baseline case required approximately 10 days of computational time. The model was first validated for its accuracy in predicting the discharge flow pattern, mass flow rate, discharge time, and the calorific value of the outlet coal mixture. Subsequently, simulations of the mixed coal discharge process under various layered stacking scenarios of Indonesian coal and Longwanggou coal were conducted. The distribution and evolution of key parameters, including flow pattern, velocity, cohesive force, and calorific value, were analyzed.

4. Results and discussion

4.1. Model validation

4.1.1. Scaling factor validation

As shown in Fig. 5, limited by computational efficiency, the L2-I1 scenario (Longwanggou coal placed in H2-H3, Indonesian coal placed in H1) is selected for scaling factor validation. Comparison results show that the simulated mass flow rate variation trends over time for scaling factors of 2 and 3 are basically consistent with the experimental results, with deviations within an acceptable range. Based on previous findings (Jiang, Li, et al., 2026), lower scaling factor yields higher computational accuracy. Comparison shows that the computational cost for k = 3 is acceptable, with a typical case requiring approximately 10 days of computation time and showing minor deviations from experimental data. In contrast, the computational time increases significantly for a scaling factor of 2 (by approximately 300%). Considering both simulation accuracy and computational cost, a scaling factor of 3 was adopted for the subsequent simulations in this work.

4.1.2. Flow pattern validation

Fig. 6 shows the experimental and numerical results of the coal particle discharge flow pattern in the silo for the L3-I2 scenario. At the same discharge time, comparing the material level height at the silo centerline, the numerical results are basically consistent with the experimental results, indicating the reliability of the model in simulating wet coal discharge.

4.1.3. Mass flow rate validation

Fig. 7(a) shows the comparison of the mass flow rate between experiment and simulation (with and without the moisture-induced cohesive force model) for the L3-I2 scenario. As shown, the results indicate that without considering the cohesive force, the overall mass

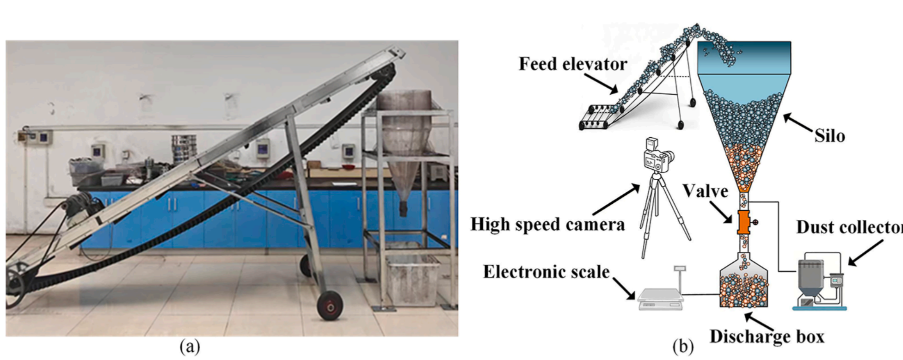

Fig. 3. Experimental system: (a) Physical and (b) Schematic diagram.

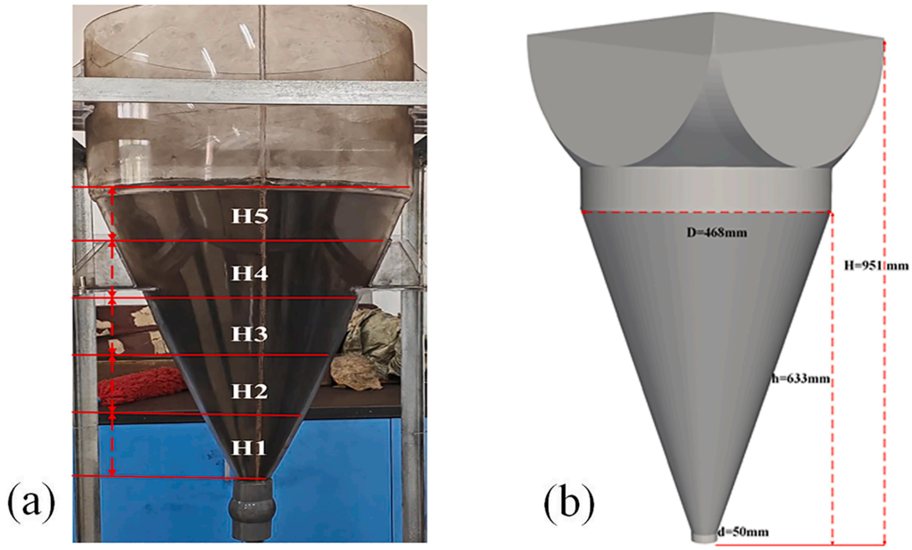

Fig. 4. Silo model: (a) Experiment and (b) Simulation.

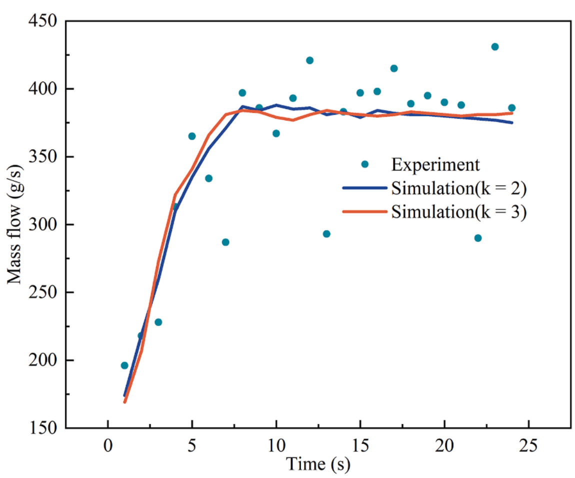

Fig. 5. Scaling factor validation.

flow rate remains at a high level, and the flow behavior of the two coal powders shows little difference. Consequently, the discharge time is also shorter. After introducing the cohesive force, the flowability differences of coal powders with different moisture contents are reflected, and the mass flow rate trend better conforms to actual discharge characteristics. From Fig. 7(b) and (c), it can be observed that by incorporating the cohesive force model, the adhesion and agglomeration of wet coal particles during the falling process are clearly visible. This shows that the established cohesive force model can effectively characterize the flowability differences of coal particles under different moisture content conditions.

From the overall discharge characteristics: the experimental total discharge mass is 30.2 kg, and the simulated total discharge mass with the cohesive force model is 29.8 kg, an error of 1.0%. The complete discharge time is 90 s for the experiment and 93 s for the simulation, an error of 3.3%. The average discharge rates from numerical calculation and experiment are 0.320 and 0.335 kg/s, respectively, an error of 4.0%. Simulation results show that because the lower part of the hopper contains high-moisture Indonesian coal with poorer flowability, the mass flow rate is initially low. As the more flowable Longwanggou coal gradually participates in the discharge, the outlet mass flow rate increases and stabilizes. In the experiment, due to the wide particle size distribution and some agglomeration, the discharge rate exhibits fluctuations of a certain amplitude. Comparing the experimental results during normal discharge with the numerical results with cohesive force, the maximum error in mass flow rate is 5.6%, within a reasonable range. This indicates the model has certain accuracy in calculating coal particle flow.

4.1.4. *Discharge time validation*

Fig. 8 shows the validation of discharge time under different scenarios for experiment and simulation. Under gravity discharge, the experimental discharge data is compared with the numerical calculation results. The maximum error between experiment and simulation is 5.2%, indicating that the mathematical model has certain accuracy in calculating wet coal particle flow.

4.1.5. *Outlet estimated calorific value validation*

Fig. 9 shows the variation of estimated calorific value of the outlet coal mixture over time for I2-L3, I1-L4 (Fig. 9(a, b)) and L2-I3, L1-I4 (Fig. 9(c, d)) scenarios, obtained by statistically determining the mass ratio of the outlet mixed coal per second and then using the lower heating value provided by the power plant. The simulated and experimentally obtained calorific values of the mixed coal are compared. Overall, the numerical results are basically consistent with the experimental trend of outlet calorific value variation. For each scenario, the maximum error between simulated and experimental estimated calorific value does not exceed 8.0%, with an average error of 2.5%. This indicates the reliability of this numerical method for predicting the mixing behavior of coal particles in silos.

4.2. *Flow pattern analysis*

To more intuitively reveal the evolution characteristics of particle flow patterns during discharge, particles are color-coded in Fig. 10, with blue representing Longwanggou coal (type 1) and yellow representing Indonesian coal (type 2). In the I4-L1 scenario, the lower Longwanggou coal discharges first rapidly, and then the entire discharge process is gradually dominated by Indonesian coal. In the I3-L2 scenario, the slight increase in the proportion of Longwanggou coal leads to its discharge within the first 20 s. In the I2-L3 scenario, mixing occurs between Longwanggou and Indonesian coal in the first 40 s, but after 40 s, Longwanggou coal is completely discharged. In the I1-L4 scenario, typical funnel flow characteristics are observed, with Longwanggou coal basically discharged after 80 s. Due to its insufficient flowability,

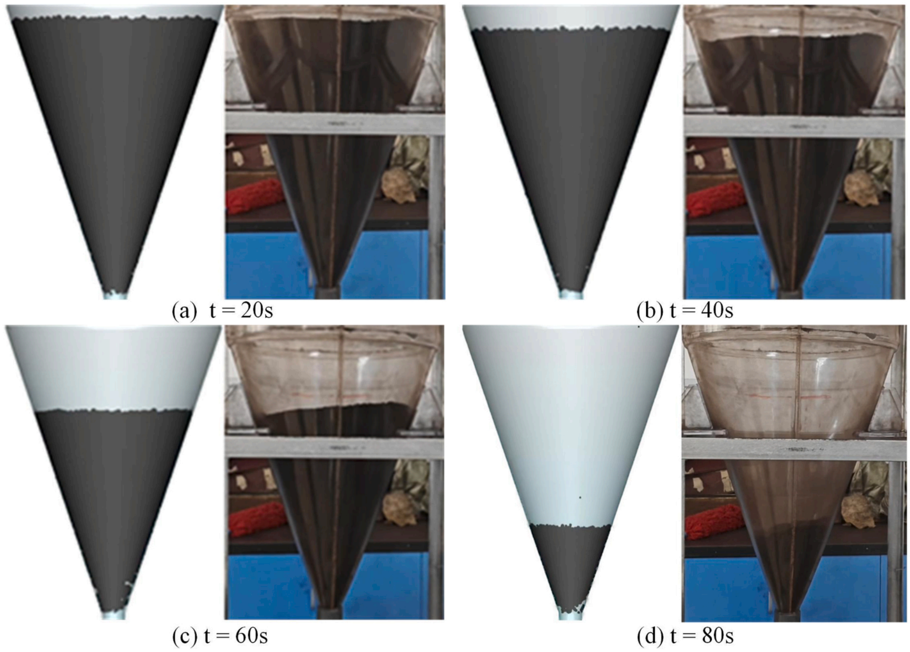

Fig. 6. Comparison of experimental and simulated flow patterns.

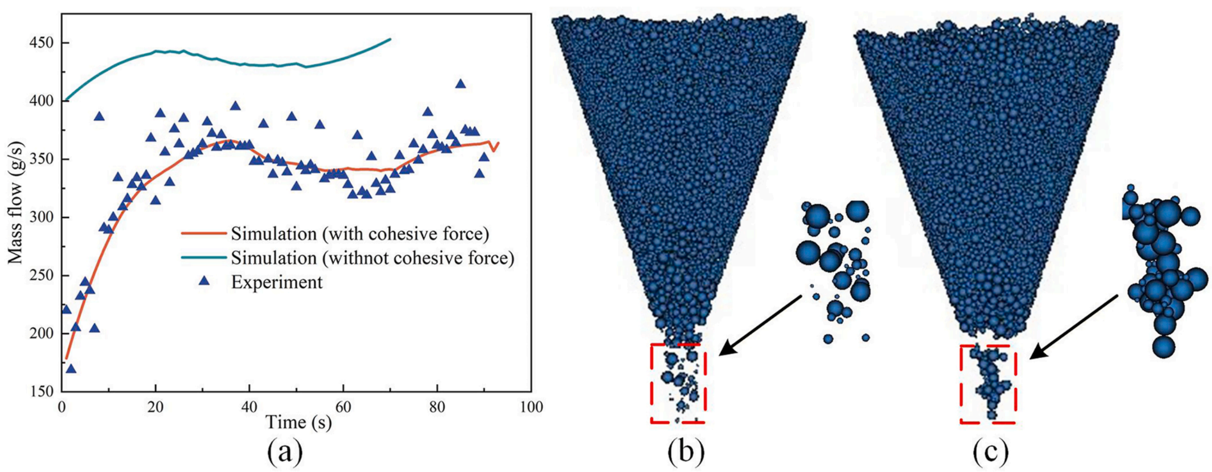

Fig. 7. Comparisons between two models: (a) variation of mass flow rate, (b) snapshot without cohesive force, (c) snapshot with cohesive force.

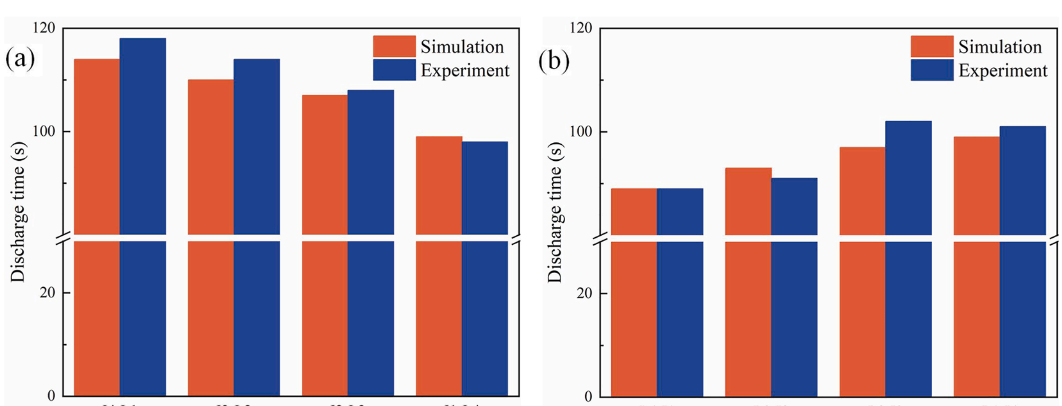

Fig. 8. Discharge time validation.

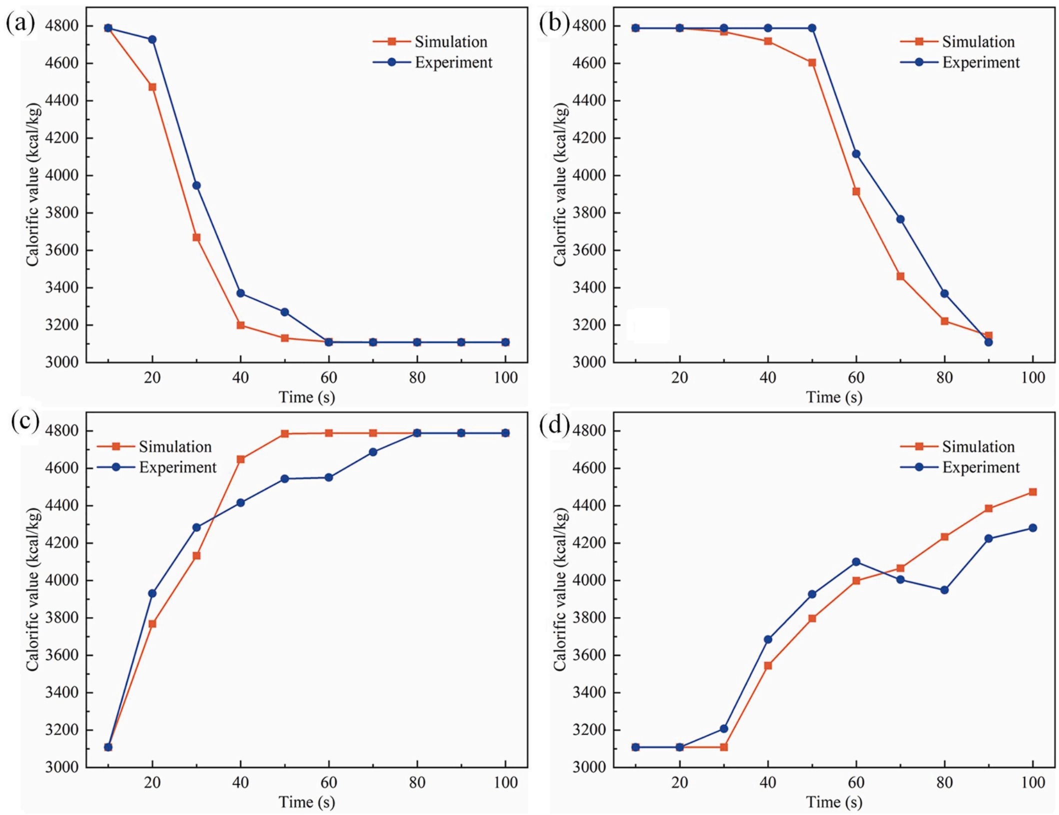

Fig. 9. Validation of simulated and experimental outlet calorific value: (a) I2-L3; (b) I1-L4; (c) L2-I3; and (d) L1-I4.

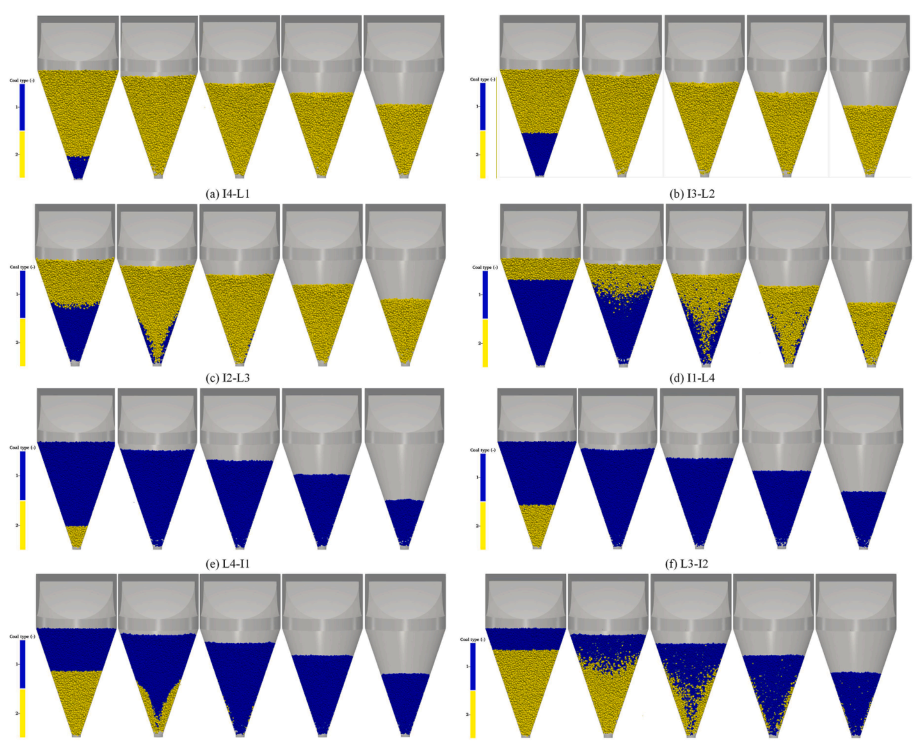

Fig. 10. Flow pattern evolution in the silo under different scenarios.

Indonesian coal struggles to follow Longwanggou coal to form efficient mixing, resulting in an overall low mixing efficiency.

In the L4-I1 scenario, the Indonesian coal discharged rapidly during the initial stage, after which the discharge process was almost entirely dominated by Longwanggou coal, exhibiting a first-in-first-out (FIFO) characteristic. A similar pattern was observed in the L3-I2 scenario, where the Indonesian coal was completely discharged within the first 20 s. The discharge process in this scenario was nearly identical to the previous one. In the L2-I3 scenario, where the proportion of Indonesian coal was significantly higher, intense mixing between the two coal powders occurred during the first 40 s of discharge. The Indonesian coal formed a typical funnel flow channel along the silo's central axis. For the L1-I4 scenario, a high degree of mixing between the coals was observed throughout the entire discharge process. The overall discharge time for this scenario was essentially the same as for the L2-I3 scenario. This phenomenon, verified by both numerical simulation and experiment, is attributed to more thorough mixing between the coal types. The more flowable Longwanggou coal was able to carry some of the Indonesian coal that tended to stagnate near the walls into the main flow, thereby enhancing the overall discharge efficiency.

Overall, the degree of mixing between the different coal powders is primarily influenced by the proportion of each coal and their flowability difference. This result not only demonstrates that the numerical simulation successfully reproduces the macroscopic phenomena observed in experiments but, more importantly, verifies the rationality of the cohesive force model. By applying differentiated cohesive forces to coal powders with different moisture contents, the model effectively reproduces the real flowability differences within the silo, ensuring consistency between the simulation results and experimental observations.

4.3. Velocity analysis

To facilitate observation of the internal flow structure, longitudinal cross-sectional views illustrating the vertical velocity distribution of particles during discharge are presented in Fig. 11. The particles are colored according to the magnitude of their vertical velocity, with blue-green indicating higher downward velocities and red indicating lower or nearly stagnant velocities. For all scenarios, the high-velocity zone was initially concentrated near the discharge outlet, while particles in the upper regions remained stagnant or moved slowly. As discharge progressed, the high-velocity zone gradually expanded upward, and the stagnant zone correspondingly shrank, indicating that upper material layers successively entered motion. Significant radial non-uniformity was observed at all cross-sectional heights. The central region exhibited a larger downward velocity, whereas particles near the walls had lower velocities and experienced stagnation, related to wall friction and inter-particle cohesive effects. In summary, the velocity distribution under all scenarios primarily formed a main flow channel along the central axis, with weaker flow in the side regions, characteristic of funnel flow. The extent and intensity of this main channel evolved throughout the discharge process.

To further investigate the velocity distribution, Fig. 12 shows the time-averaged velocity in the y-direction for particles at different height sections ($h = 0.1$, 0.2, 0.3 m) under the various scenarios. At $h = 0.1$ m, near the outlet, a clear main flow channel was evident at the central axis. Particle discharge was restricted near the walls, resulting in lower velocities. Moving horizontally towards the center, the downward velocity gradually increased, reaching a maximum near the central axis-a classic "high in the middle, low on the sides" distribution. When the lower layer

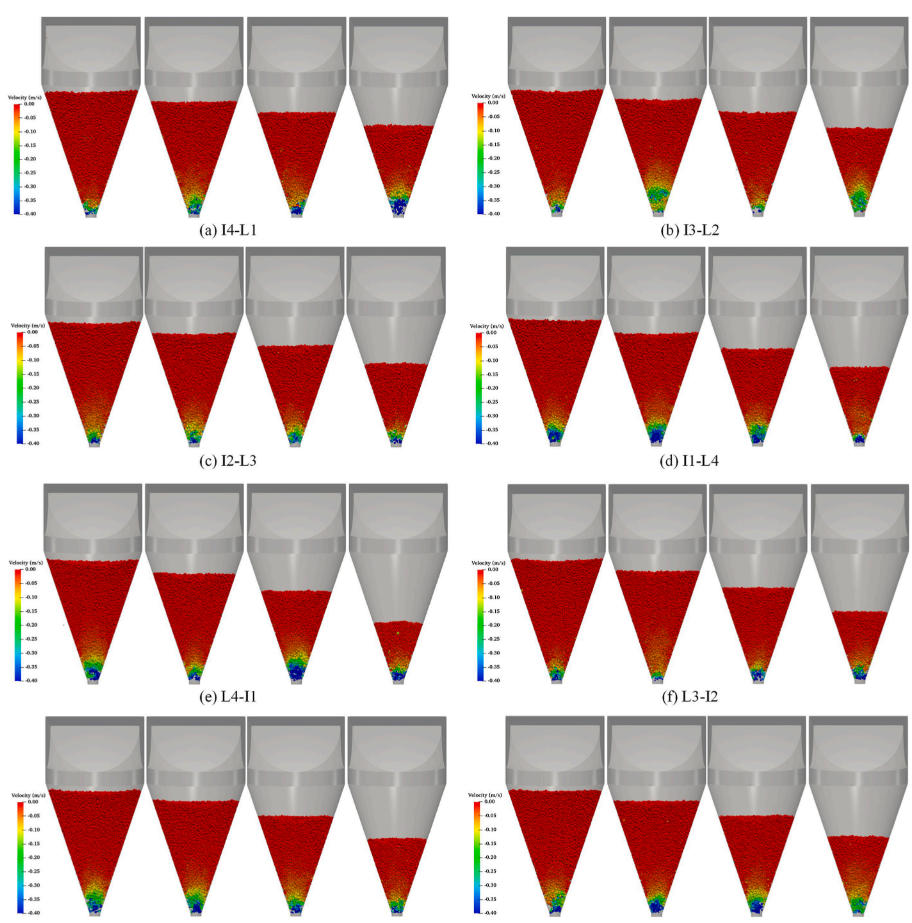

Fig. 11. Particle velocity distribution in the silo under different scenarios.

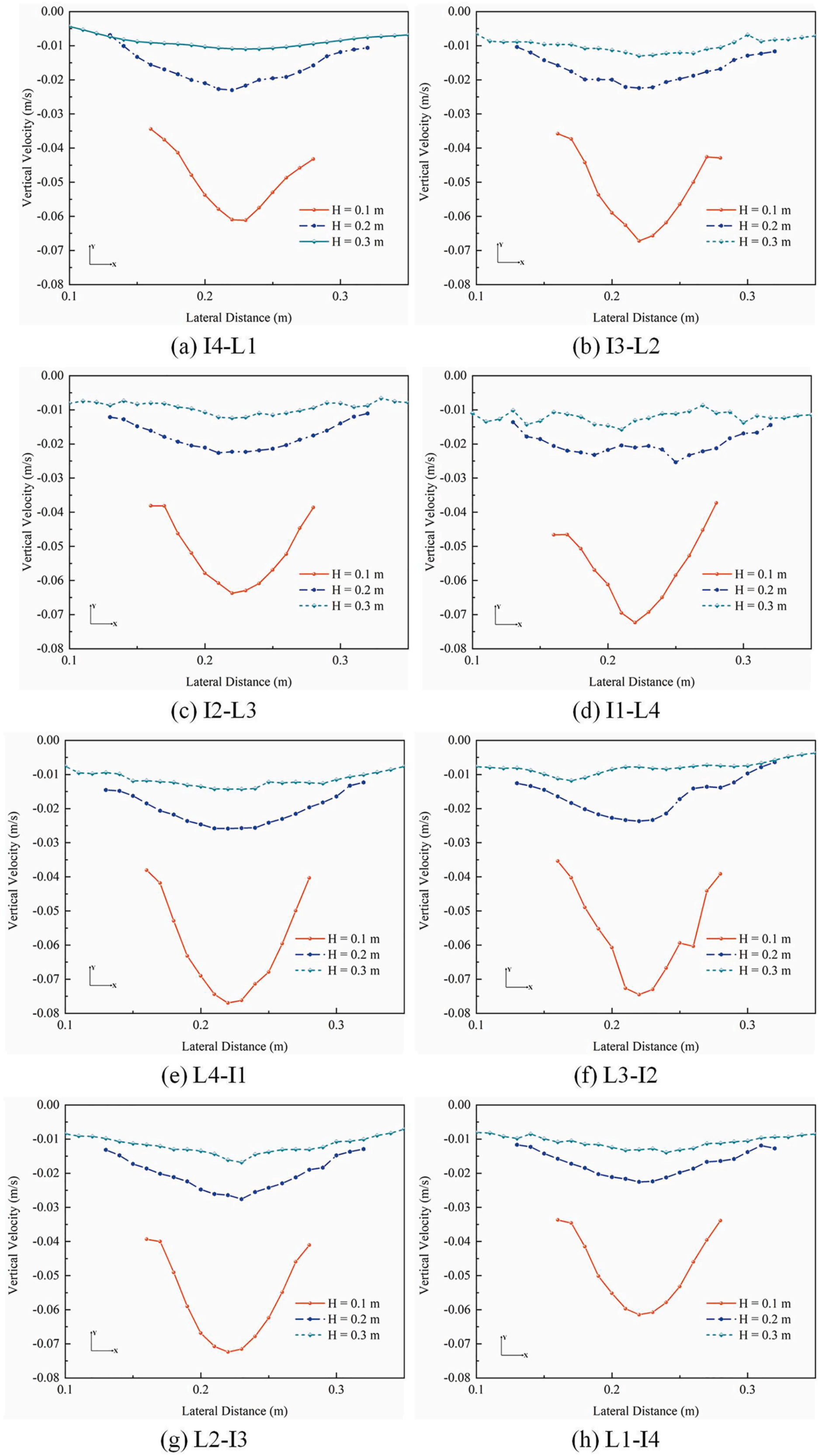

Fig. 12. Time-averaged particle velocity at different heights from the outlet.

consisted of the more flowable Longwanggou coal, the velocity peak decreased as the proportion of Indonesian coal increased. Conversely, when the lower layer was the less flowable Indonesian coal, the velocity peak increased with a higher proportion of Longwanggou coal. This indicates that the flowability difference between coal types influences the internal particle velocity distribution. At heights of 0.2 and 0.3 m, where particles are in the region of overall bed descent, the lateral velocity difference tended to moderate. The results demonstrate that the lower coal type has a decisive influence on the velocity distribution and channel morphology. A lower layer of Longwanggou coal resulted in a higher velocity peak near the outlet, whereas a lower layer of Indonesian coal led to more obvious flow obstruction and a lower central axis velocity. This confirms that the cohesive force model effectively captures the flowability differences of coal powders with varying moisture contents.

4.4. Calorific value analysis

To further analyze the variation in calorific value of the mixed coal during discharge, the mass proportion of each coal type (Indonesian and Longwanggou) flowing out per second was statistically combined with their as-received lower heating values (Indonesian coal: 3108 kcal/kg, Longwanggou coal: 4788 kcal/kg, provided by Datang South Power Plant). The theoretical calorific value of the mixed coal at the silo outlet was calculated per second for the two main stacking sequences, using the following formula:

$$Q_t = x(t) \times Q_L + [1 - x(t)] \times Q_I \tag{17}$$

where Q_t is the instantaneous mixed coal calorific value, $x(t)$ is the mass proportion of Longwanggou coal at time t, and Q_L and Q_I are the respective calorific values.

Fig. 13 shows the variation of outlet calorific value with time for these two scenarios. Different stacking sequences fundamentally altered the evolution characteristics. When the lower layer was Indonesian coal, the outlet calorific value curve showed an overall gradual increasing trend. Initially dominated by the poor-flowability Indonesian coal, the calorific value was low. As the upper Longwanggou coal gradually entered the flow channel, the calorific value increased rapidly and eventually stabilized. In scenarios with a high proportion of Longwanggou coal (L4-I1 and L3-I2), the curve approached stability within 20-30 s, indicating the rapid replacement of Indonesian coal by the highly flowable Longwanggou coal. When the proportion of Indonesian coal was higher (e.g., L2-I3 and L1-I4 scenarios), the rising phase of the curve was prolonged and exhibited multi-segment fluctuations, reflecting the alternating discharge and gradual transition of the two coals. Conversely, when the lower layer was Longwanggou coal, the outlet calorific value showed a rapid decreasing trend over time. The calorific value was initially high as Longwanggou coal occupied the outlet first, then decreased rapidly as the lower Indonesian coal gradually entered the main flow channel, finally stabilizing at a lower value. The decrease was faster in the I4-L1 and I3-L2 scenarios, stabilizing within about 20 s, indicating a rapid transition when the Longwanggou coal proportion was high. The decrease was more gradual in the I2-L3 and I1-L4 scenarios, accompanied by fluctuations, suggesting more pronounced mixing in the outlet sample at that time.

In summary, the flow characteristics of the lower coal layer have a decisive effect on the variation of outlet calorific value. When Longwanggou coal is on the bottom, the outlet calorific value shows a relatively sharp and rapid decrease at a certain stage as its proportion increases. When Indonesian coal is on the bottom, the outlet calorific value slowly rises as Longwanggou coal gradually participates in the discharge. This difference indicates that the stacking sequence of different coal types in the silo affects the evolution pattern of the discharged coal's quality. Therefore, in actual coal blending and discharge operations, the stacking sequence should be fully considered to improve the stability and uniformity of the outlet coal quality.

4.5. Cohesive force analysis

To examine the implementation of the moisture-induced cohesive force, the temporal variation in the percentage of "adhered particles" was analyzed for different scenarios. A particle was considered an "adhered particle" if it was in contact with another particle and experienced a cohesive force greater than 0.001 N (Fig. 14). Despite variations in stacking sequence and coal combination, the percentage of adhered particles remained consistently around 80% across all scenarios. This indicates that the moisture-induced cohesive force plays a dominant and stable role throughout the particle flow process, confirming the successful parameterization of the model.

To further illustrate the effect of the cohesive force on flow, the temporal variation of the average cohesive force experienced by particles inside the hopper was analyzed (Fig. 15). Overall, the average cohesive force in both main scenarios showed a decreasing trend from high to low. This is attributed to the initially densely packed, static bed of wet coal particles, where inter-particle voids are minimal and cohesive force is maximal. As discharge begins and particles flow downward, voids increase and some adhesive clusters break, leading to a reduction in the average force. For the scenarios with Indonesian coal on the bottom, the average cohesive force decreased gradually as the proportion of Longwanggou coal (with lower moisture content) increased, and the discharge time shortened, which aligns with expectations. In the scenarios with Longwanggou coal on the bottom, the situation differed. Due to the higher moisture content of Indonesian coal (moisture content of 35.1%), the cohesive force experienced by particles was greater. Consequently, as the proportion of Indonesian coal in the lower layer

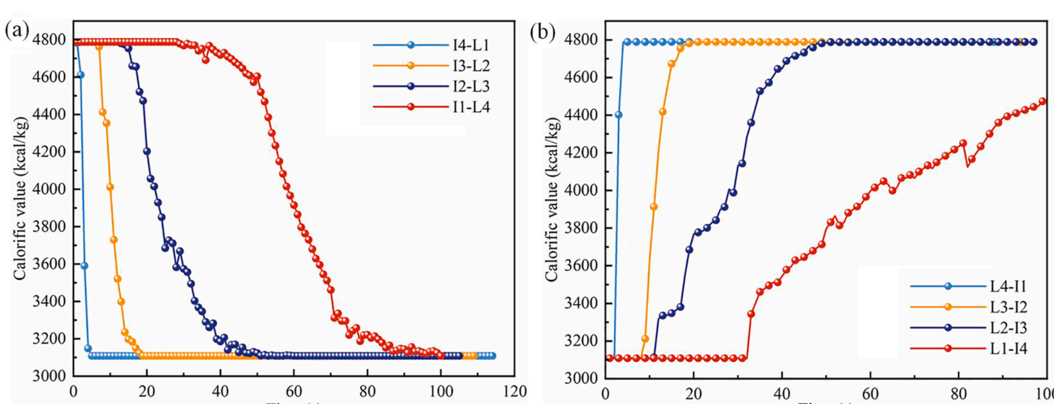

Fig. 13. Simulated estimated calorific value of outlet coal sample.

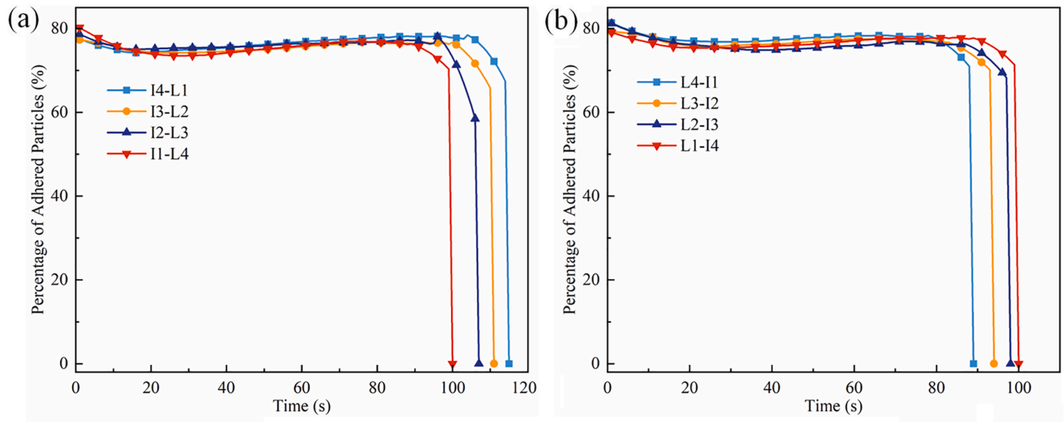

Fig. 14. Temporal variation of the percentage of adhered particles under different scenarios.

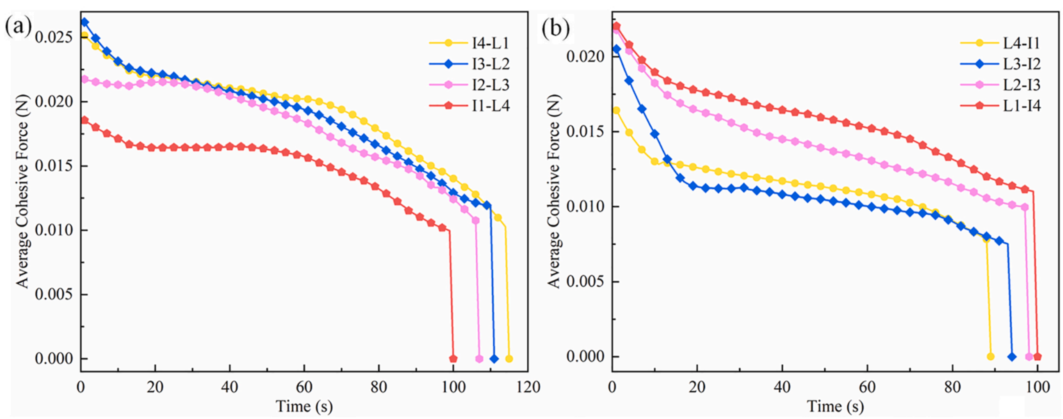

Fig. 15. Temporal variation trend of average cohesive force under different scenarios.

increased, the maximum average cohesive force also increased progressively.

5. Conclusion

This study conducted systematic numerical simulations of the layered discharge and mixing process for coals with different moisture contents in a three-dimensional silo by developing a Coarse-Grained Discrete Element Method (CG-DEM) model coupled with a moisture-induced cohesive force. The main conclusions are as follows:

(1) Model effectiveness was systematically validated through experiments. The established coupled model successfully reproduced the core physical processes of wet coal discharge. Simulation results showed good agreement with experimental data regarding discharge flow pattern, temporal variation of mass flow rate, total discharge time, and the evolution pattern of the outlet mixed coal's calorific value, with a maximum relative error within 8%. This confirms the model's capability to simulate the complex flow and mixing behavior of wet coal particles at industrially relevant scales with high precision and acceptable computational cost.

(2) The moisture-induced cohesive force dominates flow differences. The cohesive force model, constructed based on moisture content, effectively characterized the flowability differences between coal types. Simulations showed that high-moisture coal (Indonesian coal) experienced greater cohesive force, resulting in significant flow obstruction and a tendency to stagnate near walls. In contrast, low-moisture coal (Longwanggou coal) exhibited good flowability and dominated the formation of the central flow channel. Approximately 80% of particles were continuously influenced by the cohesive force throughout discharge, proving it is a key factor determining the flow morphology of wet coal.

(3) Stacking sequence determines the evolution path of coal quality. The sequence in which coal types are layered in the silo has a decisive influence on the stability of the outlet coal quality (calorific value). When the lower layer was high-moisture, low-calorific-value Indonesian coal, the outlet calorific value showed a "low first, then gradually increasing" evolution pattern, with a prolonged period of quality fluctuation. Conversely, with a lower layer of low-moisture, high-calorific-value Longwanggou coal, the pattern was "high first, then rapidly decreasing," featuring a more rapid transition but greater initial fluctuation. This provides a direct theoretical basis for mitigating feed coal quality fluctuations by optimizing stacking schemes.

(4) The flow structure exhibits significant funnel flow characteristics. Under all scenarios, funnel flow characterized by a central high-velocity downward channel and low-velocity or stagnant zones near the walls formed within the silo. The particle velocity distribution showed a radial non-uniform pattern of "high in the center, low on the sides." This flow structure was primarily determined by the flowability of the lower coal type, revealing the inherent mechanism behind wet coal's propensity for segregation and unstable discharge in silos.

In summary, the numerical model developed in this study provides a powerful analytical tool for researching the storage and conveying processes of wet particulate materials. The findings indicate that in actual power plant coal blending and feeding processes, the moisture differences between coal types and their stacking sequence must be comprehensively considered to achieve more accurate prediction and control of feed coal quality, thereby ensuring the economic and stable operation of the unit. Future work could apply this model to full-scale industrial silo simulations and further investigate the effects of auxiliary discharge measures, such as aeration and vibration, on wet coal flow.

CRediT authorship contribution statement

Haoyuan Li: Writing – original draft, Software, Methodology, Investigation, Formal analysis. **Kaixin Dai:** Visualization, Validation, Software. **Jun Xie:** Writing – review & editing, Supervision, Methodology, Funding acquisition. **Xiaole Chen:** Supervision, Funding acquisition. **Dong Li:** Supervision. **Xiaojian Xie:** Supervision. **Chuanwen Zhao:** Funding acquisition.

Declaration of competing interest

The authors declare that they have no known competing financial interests or personal relationships that could have appeared to influence the work reported in this paper.

Acknowledgements

The authors gratefully acknowledge the financial support of the National Natural Science Foundation of China (grant Nos. 52576164 and 52276120).

References

Anand, A, Curtis, JS, Wassgren, CR, Hancock, BC, & Ketterhagen, WR (2009). Predicting discharge dynamics of wet cohesive particles from a rectangular hopper using the discrete element method (DEM). *Chemical Engineering Science, 64*(24), 5268–5275.

Anand, A, Curtis, JS, Wassgren, CR, Hancock, BC, & Ketterhagen, WR (2015). Experimental study of wet cohesive particles discharging from a rectangular hopper. *Industrial & Engineering Chemistry Research, 54*(16), 4545–4551.

Chen, P, Yuan, Z, Chyang, CS, & Zhuan, F-X (2011). Sawdust discharge rate from aerated hoppers. *Particuology, 9*(3), 306–313.

Cundall, PA, & Strack, ODL (1980). Discussion: A discrete numerical model for granular assemblies. *Géotechnique, 30*(3), 331–336.

Dai, L, Yuan, Z, Guan, L, & Gu, C (2021). Investigation of wet coal flow characteristics in silos by experiments and simulations. *Asia-Pacific Journal of Chemical Engineering, 16*(3), Article e2618.

Dai, L., Yuan, Z., Guan, L., & Gu, C (2024). Discharge and mixing of moisture coal particles in silos. *Energy Sources, Part A: Recovery, Utilization, and Environmental Effects, 46*(1), 15537–15552.

Deng, Z, Fan, Y, Theuerkauf, J, Jacob, KV, Umbanhowar, PB, & Lueptow, RM (2020). Modeling segregation of polydisperse granular materials in hopper discharge. *Powder Technology, 374*, 389–398.

Garg, R, Galvin, J, Li, T, & Pannala, S (2012). Open-source MFIX-DEM software for gas–solids flows: Part I—Verification studies. *Powder Technology, 220*, 122–137.

Gou, D, & Shen, Y (2025). GPU-accelerated CFD-DEM framework for large-scale gas-solid flows with superquadric particles. *Chemical Engineering Journal, 525*, Article 170046.

Hanif, MA, Maza, D, & van der Meer, D (2025). Effect of particle shape on the discharge from a mono-layer hopper. *Granular Matter, 27*(2), 43.

Hao, Z, Fan, W, Zhang, S, Wang, Z, Dang, M, Wang, Y, Chen, Y, Zhang, Z, Tan, H, & Lin, X (2026). Influence of insert position in the hopper on powder stream mass flow rate and morphology. *Powder Technology, 467*, Article 121601.

He, Y, Hassanpour, A, Alizadeh Behjani, M, & Bayly, AE (2021). A novel stiffness scaling methodology for discrete element modelling of cohesive fine powders. *Applied Mathematical Modelling, 90*, 817–844.

Hilton, JE, & Cleary, PW (2014). Comparison of non-cohesive resolved and coarse grain DEM models for gas flow through particle beds. *Applied Mathematical Modelling, 38*(17), 4197–4214.

Höhner, D, Wirtz, S, & Scherer, V (2012). A numerical study on the influence of particle shape on hopper discharge within the polyhedral and multi-sphere discrete element method. *Powder Technology, 226*, 16–28.

Jiang, M, Li, S, Li, H, Xie, J, Liu, X, Gu, Y, Chen, X, Sun, J, & Zhao, C (2026). Numerical study of gas-solid flow and heat transfer characteristics in fluidized beds using coarse-grained CFD-DEM method. *Powder Technology, 477*, Article 122406.

Jiang, Y, Ma, T, Wu, Y, Zheng, Z, & Zhou, X (2026). Study on flow characteristics of pulverized coal in eccentrically bent coal hopper. *Advanced Powder Technology, 37*(1), Article 105132.

Jung, U, An, JH, Lim, BS, & Koh, BH (2012). Modeling discharge of pellets from a hopper using response surface methodology. *International Journal of Precision Engineering and Manufacturing, 13*(4), 565–571.

Kumar, R, Gopireddy, SR, Jana, AK, & Patel, CM (2020). Study of the discharge behavior of Rosin-Rammler particle-size distributions from hopper by discrete element method: A systematic analysis of mass flow rate, segregation and velocity profiles. *Powder Technology, 360*, 818–834.

Lu, H, Guo, X, Gong, X, Cong, X, Liu, K, & Qi, H (2012). Effects of gas type and hopper pressure on the discharge of pulverized coal. *Industrial & Engineering Chemistry Research, 51*(9), 3709–3714.

Lu, H, Guo, X, Jin, Y, Gong, X, Zhao, W, Barletta, D, & Poletto, M (2017). Powder discharge from a hopper-standpipe system modelled with CPFD. *Advanced Powder Technology, 28*(2), 481–490.

Lu, H, Guo, X, Jin, Y, & Gong, X (2018). Effect of moisture on flowability of pulverized coal. *Chemical Engineering Research and Design, 133*, 326–334.

Lu, L, Konan, A, & Benyahia, S (2017). Influence of grid resolution, parcel size and drag models on bubbling fluidized bed simulation. *Chemical Engineering Journal, 326*, 627–639.

Lu, H, Ruan, H, Poletto, M, Guo, X, & Liu, H (2023). Study on fine powder discharged from hoppers modified with insert. *Powder Technology, 423*, Article 118498.

Molerus, O. (1975). Theory of yield of cohesive powders. *Powder Technology, 12*(3), 259–275.

Queteschiner, D, Lichtenegger, T, Pirker, S, & Schneiderbauer, S (2018). Multi-level coarse-grain model of the DEM. *Powder Technology, 338*, 614–624.

Ren, G, Xu, J, Xu, J, Ouyang, Y, Ström, H, Ge, W, Sun, H, & Xiong, Q (2025). Revolution of coarse-grained CFD-DEM technology and its application in fluidized beds: A comprehensive review. *Particuology, 106*, 45–69.

Rumpf, HCH (1970). Zur Theorie der Zugfestigkeit von Agglomeraten bei Kraftübertragung an Kontaktpunkten. *Chemie Ingenieur Technik, 42*(8), 538–540.

Sakai, M, & Koshizuka, S (2009). Large-scale discrete element modeling in pneumatic conveying. *Chemical Engineering Science, 64*(3), 533–539.

Wang, S, & Shen, Y (2022). Coarse-grained CFD-DEM modelling of dense gas-solid reacting flow. *International Journal of Heat and Mass Transfer, 184*, Article 122302.

Wang, X., Zhu, HW, Shi, QF, & Zheng, N (2020). Discharge flow of granular particles through an orifice on a horizontal hopper: Effect of the hopper angle. *Chinese Physics B, 29*(4), Article 044502.

Wassgren, CR, Hunt, ML, Freese, PJ, Palamara, J, & Brennen, CE (2002). Effects of vertical vibration on hopper flows of granular material. *Physics of Fluids, 14*(10), 3439–3448.

Wu, Y., Zheng, Q, Yang, L, Zhu, H, & Yu, A (2025). Cohesive particles arch in eccentric silos. *Physics of Fluids, 37*(7), Article 073367.

Yuan, J, Jin, C, Ye, F, Hu, Z, & Chen, H (2020). Dust suppression analysis of a new spiral hopper using CFD-DEM simulations and experiments. *Processes, 8*(7), 783.

Zhang, Z, Liu, Y, Zheng, B, Li, R, & Sun, P (2021). Discharge characteristics of binary particles in a rectangular hopper with inclined bottom. *Computational Particle Mechanics, 8*(2), 315–324.

Zhao, Y, Yang, S, Zhang, L, & Chew, JW (2017). DEM study on the discharge characteristics of lognormal particle size distributions from a conical hopper. *AIChE Journal, 64*(4), 1174–1190.

Zhong, W, Yu, A, Zhou, G, Xie, J, & Zhang, H (2016). CFD simulation of dense particulate reaction system: Approaches, recent advances and applications. *Chemical Engineering Science, 140*, 16–43.

Zhu, J, Wang, K, Ma, Y, Xu, W, Long, J, & Li, X (2024). Arch formation mechanism and discharge process of cohesive fine powder in a vibrated silo. *Particuology, 94*, 373–385.